UNIVERSITY OF CALIFORNIA SAN DIEGO

Examining NRF2 expression as a potential therapy for Alzheimer's disease using an *in vitro* cell model

A thesis submitted in partial satisfaction

for the requirement for the degree Master of Science

in

Bioengineering

By

Wenyuan Wei

Committee in charge

Professor Eugene Yeo, Chair
Professor Yingxiao Wang, Co-chair
Professor Adam Engler

2020

The thesis of Wenyuan Wei is approved, and it is acceptable in quality and form for publication on microfilm and electronically:

_____

_____

Co-Chair

_____

Chair

University of California San Diego

2020

Dedication

This thesis is dedicated to my parents, my grandparents, whose unconditional love and support have led me to the place I am today.

To my dear cousin, Dr. Yuan Yang, for the invaluable guidance and encouragement she has been giving me since middle school.

For my love, Mujun. 私の側にいって本当にありがとうございます。

Epigraph

Прошу вас набраться смелости;
храбрая душа может исправить даже катастрофу.

Екатерина Алексеевна

Table of Contents

Signature Page…… iii

Dedication…… iv

Epigraph…… v

Table of Contents…… vi

List of Figures…… viii

List of Tables…… ix

Acknowledgement…… x

Abstract of the thesis…… xi

Chapter 1 Introduction…… 1

1.1 Alzheimer's disease: pathology, subtypes, pathogenesis and treatments 1

1.1.1 Pathology of AD…… 1

1.1.2 Subtypes of AD…… 3

1.1.3 Pathogenesis of AD…… 3

1.1.4 Treatments of AD…… 4

1.2 Nuclear factor erythroid 2-related factor 2: molecular mechanism, its agonist, and potential in AD treatment…… 5

1.2.1 Molecular Mechanism…… 5

1.2.3 Potential effects of NRF2 in Alzheimer's disease…… 6

1.3 Basis of this project…… 6

Chapter 2 Results…… 9

2.1 Tet-inducible gene expression construct design – First design iteration 9

2.1.1 Results from the first design iteration…… 8

2.2 Constitutive promoter construct – Second design iteration…… 12

2.2.1 Results from the second design iteration…… 12

2.2.2 Problems of the design and reasoning…… 17

2.3 Repeating experiments in HEK cells – Third design iteration…… 18

2.3.1 Results from the third design iteration…… 18

Chapter 3 Discussion…… 21

Chapter 4 Materials & Methods…… 23

4.1 cell lines, media and culture conditions…… 23

4.2 DNA constructs…… 24

4.3 Viral packaging and viral infection…… 24

4.4 qPCR analysis for plasmid gene expression confirmation…… 24

4.5 Flowcytometry analysis…… 25

4.6 Western blot sample preparation & analysis…… 25

4.7 Cell Viability test…… 25

4.8 Cellular ROS assay…… 26

Bibliography…… 27

List of Figures

Figure 1. Construct schematics and results of the first design iteration…… 11

Figure 2. Construct schematics and results of the second design iteration…… 15

Figure 3. Fluorescent microscopy images of all 12 conditions…… 16

Figure 4. alamarBlue® cell viability test results on HEK cells…… 19

Figure 5. ROS and western blot of HEK cells…… 20

List of Tables

Table 1. qPCR results for total APP expression and total NRF2 expression of the respective genotypes & conditions…… 11

Table 2. Genotype names and their respective combination of constructs…… 14

Table 3. Layout of the samples in western blot shown in Figure 2b and Figure 4d… 14

Acknowledgement

I would like to express my sincerest gratitude to Professor Eugene Yeo and all Yeo lab members for their invaluable help. I would like to especially thank Dr. Fredrick Tan for guiding and supporting me through the whole project, as well as helping revise this thesis. I would also like to thank Professor Yingxiao Wang and Professor Adam Engler to serve on my thesis committee.

Abstract of the thesis

Examining NRF2 expression as a potential therapy for Alzheimer's disease using an *in vitro* cell model

by

Wenyuan Wei

Master of Science in Bioengineering

University of California San Diego, 2020

Professor Eugene Yeo, Chair
Professor Yingxiao Wang, co-Chair

Alzheimer's disease (AD) is a neurodegenerative condition that contributes to the majority of dementia cases worldwide. The exact cause of AD remains elusive, and the study

of its disease biology is hampered by the lack of *in vitro* and *in vivo* models that are representative of the condition, and the absence of disease-modifying treatments. In this project, we attempted to use the most accurate cellular model of AD currently available to test whether an intervention that reduces oxidative stress, a common pathological feature of AD, can provide therapeutic benefits. The cellular model we used is a 3-dimensional cell matrix formed by differentiated immortalized human neural-progenitors which was previously shown to generate many key feature of AD pathobiology, such as phosphorylated Tau and Aβ aggregates. Our therapeutic intervention was the overexpression of Nuclear factor erythroid 2-related factor 2 (NRF2), a transcription factor that counters oxidative stress in normal cells and was found to ameliorate the symptoms of AD in mice. This project first made an attempt to reproduce the 3-dimensional AD cell culture model, and then test the effectiveness of NRF2 overexpression as a treatment option.

Chapter 1 Introduction

Alzheimer's Disease (AD) is a neurodegenerative condition that is gaining attention globally (1,2). It is one of the leading causes of dementia – up to 50% to 70% of all dementia incidences (1). Onset time of AD is usually late in life, with an average onset age of over 65 years in the United States (2). Nevertheless, there are still incidences of AD development at a much earlier ages. The first identified and reported occurrence of AD was in 1907. However, research on AD biology, its pathogenesis did not make much progress until about four decades ago (2). There is currently still no disease-modifying treatment to AD (1–4).

The expression of Nuclear factor erythroid 2-related factor 2 (NRF2), a leucine-zipper transcription factor of cap 'n' collar (CNC) subfamily that regulates genes in cellular homeostasis, represents one potential therapeutic intervention (5,6). A major function of NRF2 is resolving oxidative stress, which is common to many neurodegenerative conditions, in order to limit physical damage to cellular proteins and DNA. NRF2 also upregulates autophagy, inflammation response, mitochondrial biogenesis, angiogenesis and apoptosis (6,7). Not surprisingly, NRF2 knock-out mice are more prone to chemical toxicities and diseases that induce oxidative stress (8). NRF2 may also protect against aging and age-associated disease (5). Here, we examine the benefit of NRF2 expression in ameliorating the molecular feature of AD pathobiology using an *in vitro* cell culture model.

1.1 Alzheimer's disease: pathology, subtypes, pathogenesis and treatments

1.1.1 Pathology of AD

There are two facets of AD pathology: 1) behavior and cognitive impairment and 2) the underlying molecular process that drives disease pathology. As previously mentioned, the most defining consequence of AD is dementia, in which there is a defect in the acquisition of new information (2). Other symptoms include an inability to properly plan and execute, an inability to generate comprehensive speeches, and an inability to identify objects. Since AD

is not the sole cause of dementia, in order to distinguish AD from other neurodegenerative conditions that also lead to dementia, one has to further explore the molecular phenotype of AD.

The major molecular phenotypes associated with AD are amyloid-beta (Aβ) plaques and neurofibrillary tangles (NFT). The presence of these pathologies lead to synaptic and neuronal loss and eventually brain atrophy (1,2).

Aβ is a natural byproduct of amyloid precursor protein (APP) metabolism, which is cleaved fragment derived from a region near the APP transmembrane region. Aβ is deposited extracellularly and is actively cleared from the cerebrospinal fluid (CSF); Aβ can have various lengths, but the most abundant is 40 amino acid in length ($A\beta_{40}$). By contrast, the Aβ plaque is the extracellular accumulation of misfolded Aβ variants, composed primarily of $A\beta_{40}$ and/or fragments that are 42 amino acids in length ($A\beta_{42}$). These mis-folded Aβ peptides have a high tendency to aggregate and form insoluble filaments. It is believed that misfolded $A\beta_{42}$ is more pathogenic due to its intrinsic insolubility and high rate of fibrilization (1). However, recent studies have shown that certain ratios of $A\beta_{40}$ to $A\beta_{42}$ in Aβ plaques can be more toxic than others, even more so than pure $A\beta_{42}$ alone (9). Such insoluble protein aggregates can block synaptic transmission and lead to synaptic loss (2).

NFTs are mainly composed of hyper-phosphorylated Tau, a microtubule-associated protein that is found in neurons. It functions in microtubule assembly to facilitate proper movement of the cytoskeletal network (10). The interaction of Tau with the microtubule network is regulated by phosphorylation at the KXGS motifs within microtubule-binding repeats. Phosphorylation at this location significantly reduces its ability to bind to microtubules (11). The mechanism enables the a highly dynamic assembly and disassembly of microtubules. Tau thus also aids in neurite outgrowth and axon transport (12,13). However, phosphorylation at other non-physiological locations, especially Ser422, was

shown to render Tau highly fibrillogenic and strongly promote the formation of NFTs (14). Additionally, other studies have indicated that truncated Tau at Asp421 (Tau_{D421}) increases the rate of firillogenesis (15,16). Tau with improper phosphorylation is referred to as hyper-phosphorylated Tau. Due to the highly fibrillogenic nature of hyper-phosphorylated Tau, its accumulation will form NFTs and interfere with neuron health and integrity.

1.1.2 Subtypes of AD

With the current understanding of AD pathogenesis, only a small fraction of AD incidents can be explained by heritable traits, which are categorized as Familial Alzheimer's Disease (FAD); the origin of the vast majority of AD incidences is still unknown and those are referred to as Sporadic Alzheimer's Disease (SAD).

FAD only consists of less than 0.5% of total AD incidences (1). FAD is inheritable and has a much earlier onset time in life, usually between 30 to 50 years of age (1,2). These patients usually have defining mutations in APP, and/or presenilin 1/2 (PSEN1/PSEN2), the γ-secretases that are responsible for the cleavage of APP during its metabolism.

SAD, as the name indicates, is sporadic and lacks clear genetic hallmarks. It is believed that both environmental and genetic factors contribute to the development of SAD (1,2,17).

1.1.3 Pathogenesis of AD

The exact pathogenic mechanisms of AD are still elusive, but several hypotheses have been proposed. The most well-accepted hypothesis is the "amyloid cascade hypothesis". It states that misfolded Aβ peptides not only initiate the amyloid plaque, but can also trigger NFT formation (18,19). As such, Aβ generation and aggregation are the causative agents for AD. Nevertheless, contrary evidence using in mouse model shows that the formation of Aβ plaques does not necessarily induce Tau-hyperphosphorylation, nor does such aggregation

cause neuronal loss (20). Of course, this is based on the assumption that AD mouse models can recapitulate human AD biology.

An alternative to the amyloid cascade hypothesis is the "Tau hypothesis". Supporters of this hypothesis claim that Tau, rather than Aβ, is the causative factor of AD pathogenesis. Studies have given insights into the correlation of Tau aggregation and AD pathological development (21,22). Moreover, others have found that Tau aggregation proceeds the formation of Aβ plaques (23,24).

A third emerging hypothesis is called "mitochondrial cascade hypothesis". This hypothesis, unlike the previous two, does not propose a pathological molecule to be the causative agent of AD. It stems from observations that mitochondrial function decreases with age, and the observed decline is worse in AD patients (25–27). Here, it is believed that the cause of AD, especially for SAD, is the lack of mitochondrial function and leads to the buildup of reactive oxidative species (ROS). Mitochondrial function is linked to APP expression and processing. Loss of mitochondrial function might therefore promote Aβ plaque formation (28–30). Once insoluble Aβ begins to deposit, the disease outcomes would be similar to that of the "amyloid cascade hypothesis".

1.1.4 Treatments of AD

There is currently no cure for AD. With that said, however, five treatments that address AD symptoms have been approved by FDA. Broadly speaking, there are two types of drugs. The first type are three drugs categorized as "cholinesterase inhibitor": donepezil, galanthamine and rivastigmine (31). By inhibiting acetylcholine esterase (AChE) and butyrylcholine esterase (BuChE), enzymes that are believed to promote Aβ deposition and aggregation, these drugs can offset AD symptoms to some extent (32). The second type is a drug called memantine, which is a "partial antagonist of N-methyl-D-aspartate (NMDA) Receptor" (33). While NMDAR activity is pivotal in maintaining neural transmission, hyper-

active NMDAR is observed to cause neural excitotoxicity and lead to neuronal death (34). Memantine is viewed as a viable drug to block excessive NMDAR activity: memantine is only effective in blocking hyper-active but not normal NMDAR(35). It has been shown that, in an AD mouse model, memantine has neuroprotective effects against neurotoxicity induced by Aβ (36–38). In clinical trials, patients that were administered memantine also showed statistically significant improvement on behavior assessments, as compared to patients administered with placebo (39,40). The fifth drug that is FDA-approved is a combination of donepezil and memantine.

1.2 Nuclear factor erythroid 2-related factor 2: molecular mechanism, its agonist, and potential in AD treatment

1.2.1 Molecular mechanism

The activity of NRF2 is closely regulated by Kelch-like erythroid cell-derived protein with CNC homology-associated protein 1 (Keap1). Keap1 is a redox-sensitive adaptor for Cul3 E3 ubiquitin ligase; it binds to the Neh2 motif on NRF2 and marks it for degradation by the Cul3 E3 ubiquitin ligase (41–44). The binding of Keap1 to NRF2 also locks NRF2 in cytoplasm, preventing NRF2 from travelling into the nucleus (45). In the presence of reactive oxidants, Keap1 is oxidized and inactivated, allowing NRF2 to translocate into the nucleus and activate transcriptions of its downstream genes. NRF2 controls expression of a number of ROS-detoxifying enzymes such as glutathione peroxidase 2 (46). It also regulates the glutathione antioxidant system by controlling the catalytic and modifier subunits of glutamate-cysteine ligase, the key component of the system (47).

Keap1 activity can also be modified by adding exogenous chemicals, though the mechanisms through which these compounds act differ. For example, tert-Butylhydroquinone (tBHQ) can bind to Keap1 and cause a conformational change of Keap1, thus preventing ubiquitination of NRF2. Others such as toxic heavy metal ions can directly dissociate NRF2

from Keap1 (6). Most of the substances that are capable of inducing oxidative stress can activate NRF2; however, many of these substances are toxic even at low levels. Sulforaphane is a NRF2 agonist that can be found naturally in vegetables and has been shown to be non-toxic at low concentration(48,49). Sulforaphane binds to Keap1 and modifies its cysteine residue, which inactivates Keap1, and stops the degradation of NRF2 (50).

1.2.2 Potential effects of NRF2 in Alzheimer's disease

There has been researches relating Aβ and hyper-phosphorylated Tau, directly or indirectly, to oxidative stress in AD models (4,51). Since NRF2 can reduce oxidative stress, we hypothesize that upregulation of NRF2 expression and activation of its downstream target genes can help slow down Aβ plaque formation and NFT formation.

In fact, studies have shown that upregulating NRF2 expression is effective in alleviating AD syndromes in mouse models (52–56). Sulforaphane, specifically, was used in studies to address AD biology both using *in vitro* and *in vivo* mouse model (57–60). Those studies indicate that upregulation of NRF2 can be protective against AD.

1.3 Basis of this project

One drawback of current *in vitro* cell culture models is that they do not faithfully replicate AD biology. Besides primary cells obtained directly from AD patients, the closest cell lines researchers can obtain are human neuronal cancer cell lines like SH-SY5Y cells, or neuronal cells from other animals such as PC12 cells.

In 2014, a cell model was created using ReNcell VM (ReNcell) and has been touted as a new representative AD model. Choi *et al.* from Harvard Medical School published a paper, in which they described an *in vitro* three-dimensional AD model using ReNcells that could reproduce a number of key features in AD patients (61). ReNcell is a human-derived immortalized neuro progenitor cells (NPC) that is capable of differentiating into a rather comprehensive neural network of neurons and glia when cultured in three-dimensions.

Compared to the previously models, the use of ReNcell has a number of advantages: 1) Though immortalized, it is not a cancer cell line, and maintains stem-cell like properties, 2) it is human derived, which naturally gives more credibility than studies performed using other animal-derived cell lines, 3) since it is immortalized, ReNcells are easier to culture and handle than both primary cells and induced Pluripotent Stem Cells (iPSCs) and 4) it is capable of giving rise to a more complete neural network, which better represents natural condition in brain than neuron-only culture or artificially-mixed neuronal co-cultures.

In this model, mutant version of both APP and PSEN1 were introduced into ReNcells prior to differentiation. The mutant APP contained a London mutation (V717I), one of the most common APP mutation worldwide, and the Swedish mutation (KM670/671NL). Together, this APP (*Swe/Lon*) can reproduce amyloid pathology in a mouse model (62,63). The mutant PSEN was ΔE9 (T291_S319del), a mutation that lacks exon 9 of PSEN1(64). In a 3- to 8-week period, expression of pathological mutant proteins in differentiating 3-dimensional ReNcell cultures could produce features of AD samples, namely amyloid beta plaques, and NFTs.

Besides being representative of AD pathology, there are two other defining advantages of the ReNcell model. First, ReNcells are commercially available, which is much more accessible than human primary cells or iPSCs. Second, all mutant genes are introduced with constitutive promoters, making the induction of pathological gene expression easy to control.

However, there are several drawbacks to the use of ReNcells or the method of generating AD pathology that must also be mentioned. First, the mutant genes expressed in this cell culture model are derived from FAD patients, which represent only a small fraction of observed AD cases. Second, constitutive expression of these mutant APP/PSEN1 proteins may poorly represent AD pathology in the brain and may not occur in the vast majority of

sporadic cases. Third, the cost and time spent generating the ReNcell model can be quite significant.

Despite these drawbacks, this project used ReNcells with some improvements to the experimental protocol, to test the efficacy of NRF2 on AD pathology.

Chapter 2 Result

2.1 Tet-inducible gene expression construct design – First design iteration

One of the main weakness of the design described in Choi *et al.* is that all pathogenic genes are expressed under a constitutive promoter, which immediately start expressing upon their introduction in ReNcells. This immediate expression in the neuronal stem cell state may not be truly representative of AD biology, which occurs in a more differentiated cell state. To circumvent this issue, we chose to drive gene expression with minimal CMV promoter with Tet-inducible repeats to achieve inducible control of gene expression. APP with *Swe/Lon* mutations and mutant PSEN1 (ΔE9) were co-expressed from the same transcript via an intermediate IRES sequence (AiP), and mCherry was expressed from on a separate promoter downstream of AiP open reading frame (Figure 1a). The mCherry reporter was used to select cells (using Fluorescent Activated Cell Sorting) for stable integration of the transgene construct. A control construct that expressed only mCherry without AiP was also created (mC) (Figure 1a). The treatment being considered is NRF2 expression. The NRF2 coding sequence was also cloned downstream of a Tet-inducible promoter, but with citrine as the fluorescent marker (NRF2) (Figure 1a).

2.1.1 Results from the first design iteration

A flowcytometry analysis was carried out to understand the composition of cell population in terms of stemness and lentiviral infection efficiency (Figure 1b). Sex-determining region Y box 2 (Sox2) is a transcription factor essential for maintaining neural stem cell self-renewal (65). It is used to determine the stemness of the population. All groups showed mixed stemness, indicating inhomogeneous population of NPCs with potentially partial differentiation. As this inhomogeneity was observed even in wildtype ReNcell population, it was likely not caused by introduction of lentivirus, or pathogenic transgene AiP and likely due to instability as a result of culture condition. While mC showed a uniform high

level of mCherry fluorescence, AiP had a long tail of less fluorescent population. This indicated that the infection efficiency of AiP lentivirus was low, or that the AiP construct was not functioning as expected.

A qPCR analysis was then done to ensure that our AiP construct was indeed expressing pathogenic AiP. Our qPCR primers targeted a sequence in the APP coding region. We discovered that when doxycycline was added to induce transgene expression, the stable AiP cell lines had comparable level of APP mRNA production compared to unmodified wildtype cells. These data indicated that the transgene was not expression any additional APP and that it was defective in expression. By contrast, if we used the same DNA construct prior to its viral packaging and used lipofectamine to introduce it into cells, qPCR analysis showed a roughly 22-fold increase in APP mRNA production (Table 1). Together, these data indicated that there may have been a problem with lentiviral packaging of AiP

By contrast, when cells were infected with NRF2 lentivirus and doxycycline induced, an 174-fold increase in mRNA production over wildtype was observed. Cell cultured without doxycycline were only 11-fold over wildtype (Table 1). Such a result confirmed the proper integration and inducibility of the NRF2 transgene.

Since the Tet-inducible promoter in NRF2 construct was functional, problems encountered in the AiP lentiviral packaging might not be the result of issues with the Tet-responsive promoter, which has repetitive DNA operator elements. Another significant difference between the two constructs is the size of the insert. While AiP construct was 15.7Kb in size, NRF2 construct was 13.4Kb. The large size of the AiP construct might have impacted the packaging process. With this in mind, a second design iteration was initiated.

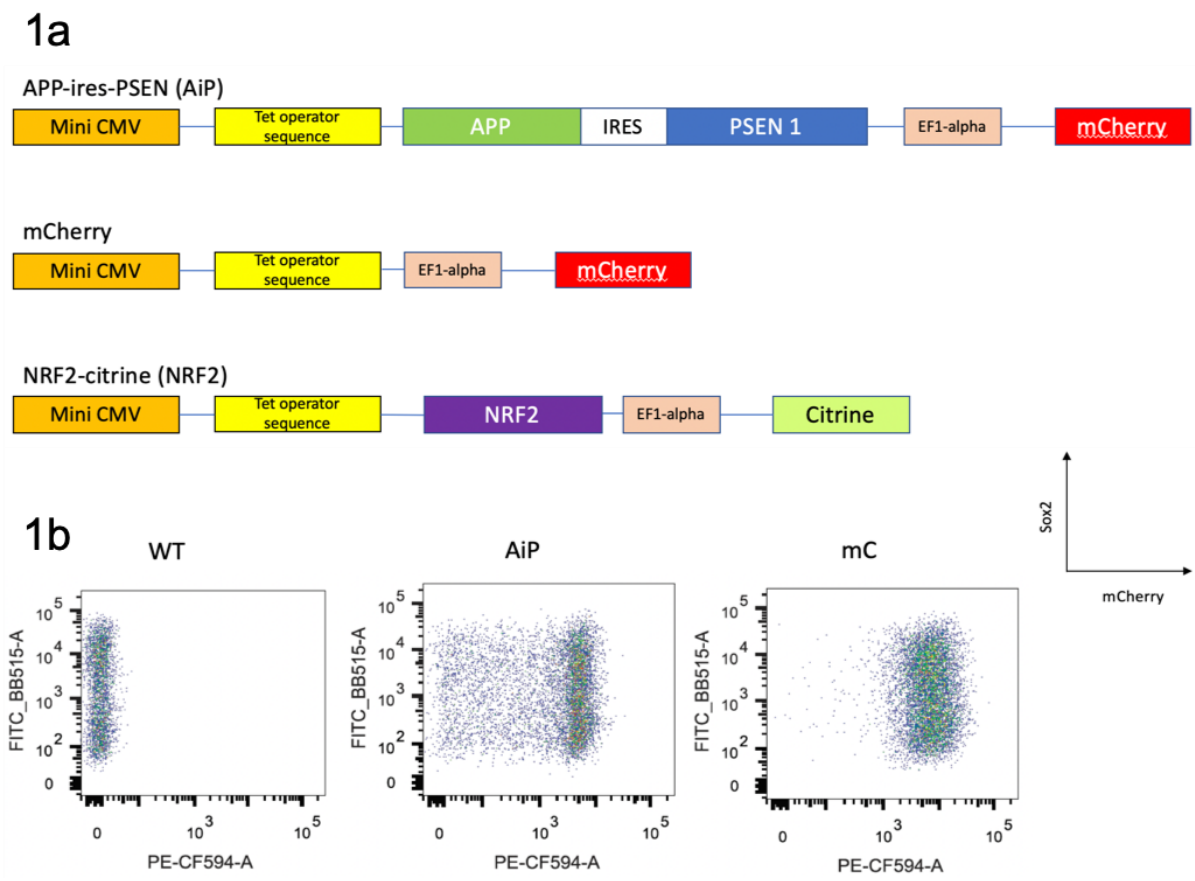

Figure 1. Construct schematics and results of the first design iteration. 1a: construct schematics of the first design iteration. 1b: flowcytometry result of three cell populations; WT: wildtype ReNcells with no plasmid incorporated; AiP and mCare: ReNcells with the same-name plasmid incorporated, respectively. X-axis: mCherry fluorescence, channel: BD Horizon PE-CF594. Y-axis: Sox2 expression in Alexa488 fluorescence, channel FTTC-BB515.

Table 1. qPCR results for total APP expression and total NRF2 expression of the respective genotypes & conditions.

Genotype & Delivery Method	ΔΔCT for APP
AiP via lipofectamine + Dox	4.49
AiP via lentivirus + Dox	0.85

Genotype	ΔΔCT for NRF2
NRF2 via lentivirus	3.50
NRF2 via lentivirus + Dox	7.44

2.2 Constitutive promoter construct – Second design iteration

In order to address the problems encountered in the first design iteration, we replaced the Tet-inducible promoter with a constitutive mouse phosphoglycerate kinase promoter 1 (PGK). The change was made to ensure expression of AiP transgenes, even though it compromised the ability to induce gene expression at a later development stage. The PGK promoter was chosen because among the common constitutive promoters used in mammalian cells, it has a lower level of expression (66). In addition, since the transgene would be constitutively expressed, the mCherry sequence was moved and cloned downstream of AiP, so that it could be co-expressed from the same transcript via an additional IRES sequence. These changes allowed the lentiviral construct to decrease in size from 15.7Kb to 14.4Kb.

Since Tau also plays a major role in AD biology, a new construct containing a truncated Tau sequence (1n4r- Tau_{D421}) was also made as an alternative to AiP for inducing AD biology in ReNcells (Figure 2a). As previously mentioned, Tau_{D421} was shown to have a higher affinity in aggregation and could result in a better representation of tau-pathology than wildtype Tau protein.

2.2.1 Results from the second design iteration

The new constructs were used to infect 12-day differentiated ReNcells that were either wildtype or NRF2-incorporated. A total of 12 conditions were made; their names and respective genotypes are described in Table 2. All cells were allowed to differentiate until day 22 before lysed for western-blot analysis (Figure 3). The lentiviral packaging problem was not observed in this iteration. Fluorescent signal was observed from all conditions containing AiP construct, as mCherry gene was attached directly after AiP, which confirmed the expression of AiP as well. Noticeably, while virus containing Tau_{D421} protein had a very high infection efficiency (Tau-mCherry in 3a, 3b, 3c), the infection efficiency of virus containing AiP was much lower (AiP-mCherry in 3a, 3b, 3c).

When comparing culture density between groups, increased cell death was observed across all groups containing pathogenic transgenes. Cells containing pathogenic transgenes also showed morphological difference from their perspective wildtypes; elongation of cell body and extensive growth of axons were observed. This may or may not be a result of lower cell counts.

In order to understand the effects of AiP on ReNcells, a quick cell viability test was done to assess the impact of AiP on cell viability (Figure 2b). The result showed a promising trending of NRF2 enhancing cell viability.

A western blot probing for NRF2 was carried out. Layout of samples is shown in the table (Table 3). The rationale is that with the presence of oxidative stress from pathogenic transgenes, endogenous NRF2 would be activated. NRF2 overexpression from NRF2 transgene construct would synergize with endogenous NRF2 to yield a higher level of NRF2 protein. Difference between NRF2-D-AiP, NRF2-D-Tau and NRF2-D-AiPT would show the extent of oxidative stress exerted by each pathogenic transgene condition. With sulforaphane, which activates NRF2 by inactivating Keap1, on the other hand, all NRF2-Dox samples should show comparable NRF2 protein level that are higher than the rest of the samples: as Keap1 is inactivated by sulforaphane, all NRF2 mRNA should be converted to NRF2 protein. It was expected that without sulforaphane induction, NRF2-D-AiP, NRF2-D-Tau and NRF2-D-AiPT would have higher NRF2 protein level, compared to the rest of the samples.

However, only sulforaphane and doxycycline double induced cells had visible NRF2 bands (Figure 2c). The result indicated that the repression of NRF2 by Keap1 was strong, and could only be relieved by the presence of sulforaphane. Moreover, endogenous NRF2 protein could not be detected even with sulforaphane given its low level of expression and the presence of an NRF2 transgene was required to boost NRF2 expression to detectable levels. To better assess the difference between only the NRF2-Dox samples, A second western blot

was also done, with only doxycycline-induced samples (Figure 2d). All lanes showed comparable signal levels. This indicated that the expression of AiP, Tau or AiP and Tau had very limited impact on activating NRF2-related pathway.

Table 2. Genotype names and their respective combination of constructs.

Genotypes	WT	AiP	Tau	AiP+Tau
WT	WT-WT	WT-AiP	WT-Tau	WT-AiPT
NRF2	NRF2-WT	NRF2-AiP	NRF2-Tau	NRF2-AiPT
NRF2+Dox	NRF2-D-WT	NRF2-D-AiP	NRF2-D-Tau	NRF2-D-AiPT

Table 3. Layout of the samples in western blot shown in Figure 2b and Figure 4d.

1	2	3	4	5	6	7	8	9	10	11	12
WT-WT	NRF2-WT	NRF2-D-WT	WT-AiP	NRF2-AiP	NRF2-D-AiP	WT-Tau	NRF2-Tau	NRF2-D-Tau	WT-AiPT	NRF2-AiPT	NRF2-D-AiPT

2a APP-ires-PSEN (AiP)

Tau

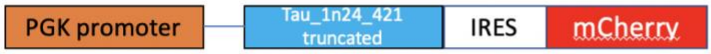

NRF2-citrine (NRF2)

2b

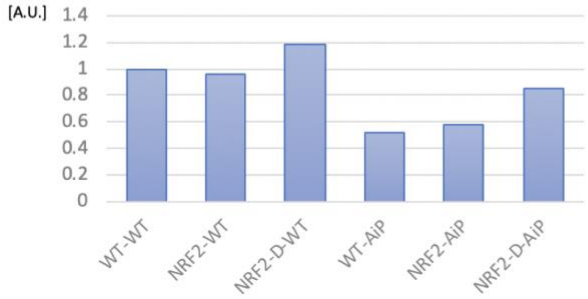

2c

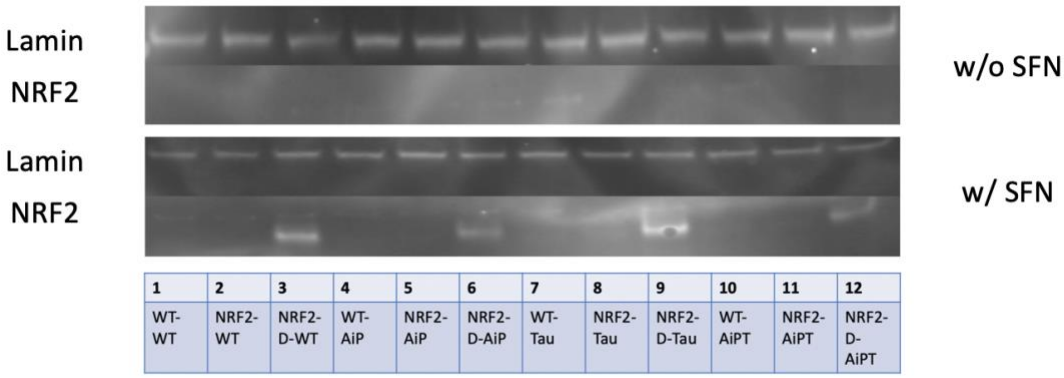

1	2	3	4	5	6	7	8	9	10	11	12
WT-WT	NRF2-WT	NRF2-D-WT	WT-AiP	NRF2-AiP	NRF2-D-AiP	WT-Tau	NRF2-Tau	NRF2-D-Tau	WT-AiPT	NRF2-AiPT	NRF2-D-AiPT

2d

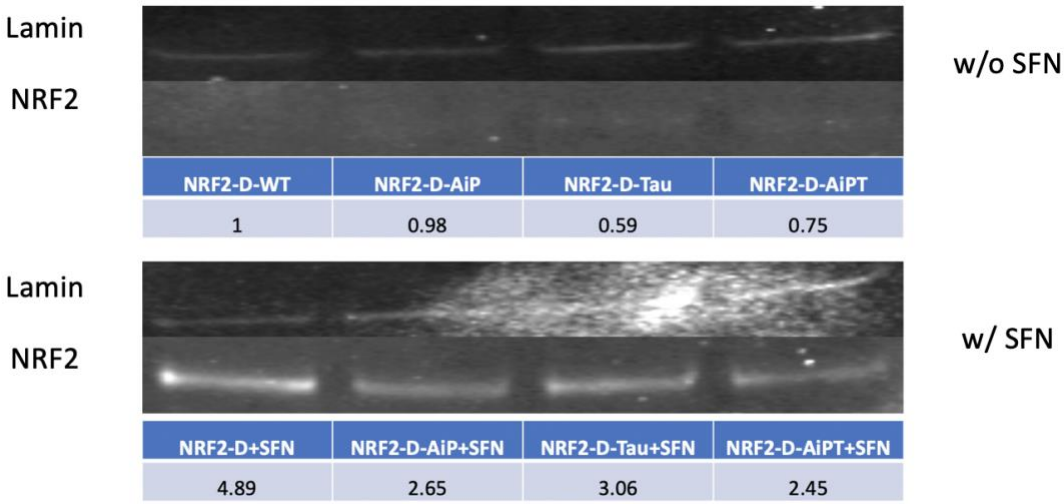

NRF2-D-WT	NRF2-D-AiP	NRF2-D-Tau	NRF2-D-AiPT
1	0.98	0.59	0.75

NRF2-D+SFN	NRF2-D-AiP+SFN	NRF2-D-Tau+SFN	NRF2-D-AiPT+SFN
4.89	2.65	3.06	2.45

Figure 2. Construct schematics and results of the second design iteration. 2a: construct schematics of the second design iteration. 2b: alamarBlue® cell viability test result of 6 different cell populations. Arbitrary Units = [A.U] 2c: western blot result of all 12 test groups with/without sulforaphane; layout of samples corresponds with the chart below. 2d: western blot result of only doxycycline-induced groups with/without sulforaphane; layout of samples corresponds with the chart below; intensity fold changes are labeled below, normalized to NRF2-D-WT.

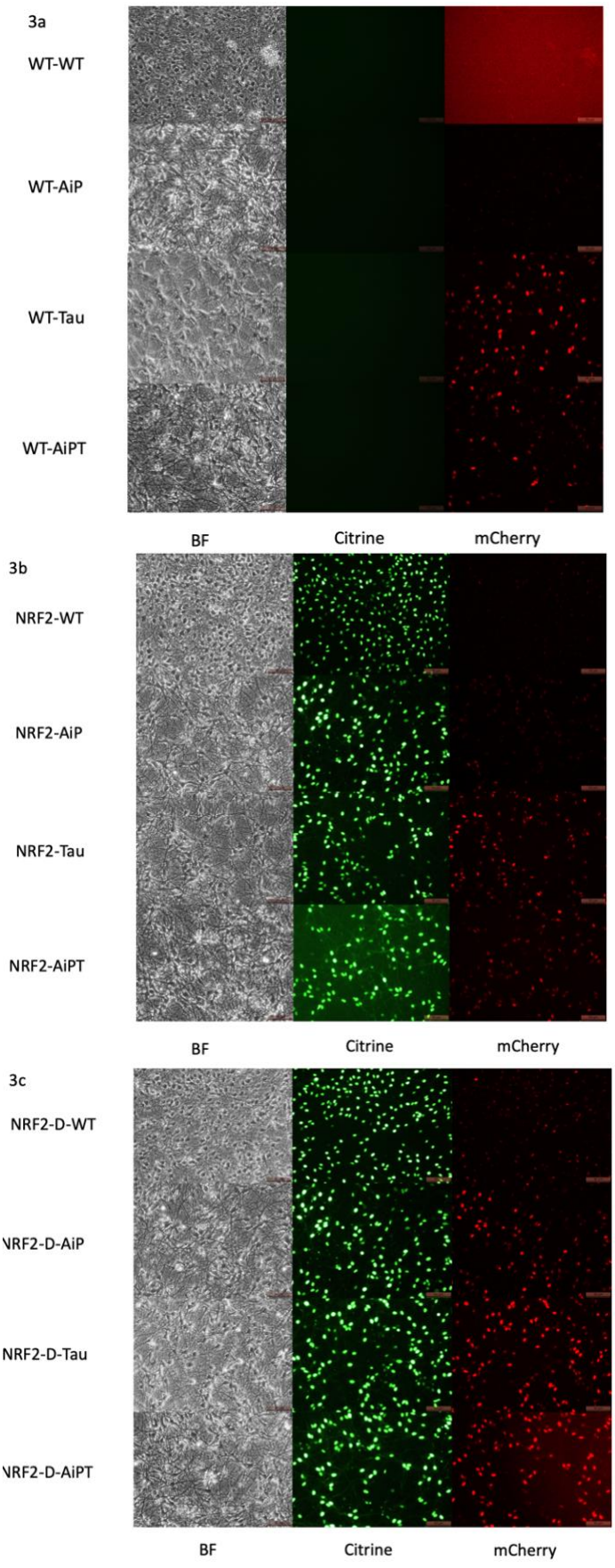

Figure 3. Fluorescent microscopy images of all 12 ReNcell conditions described in Table 2. BF: bright field.

2.2.2 Problems of the design and reasoning

Although a set of preliminary result was generated using ReNcells, the end point was never reached due to the COVID-19 pandemic that was, and still is spreading as of right now. As a planned differentiation protocol takes 6 to 8 weeks, with constant feeding and monitoring, it was impossible to maintain the cultures. Thus, existing trials was harvested immediately and no further trial was initiated when the state stay-at-home order was issued.

Unfortunately, there is still no decisive evidence on how lentiviral packaging failed in our first generation AiP constructs. Based on our observations in the first and second iteration, not only could lentiviral packaging of AiP construct be defected, but AiP gene cassette could also be very hard to express. This was supported by the observation that even with a constitutive promoter like PGK, the fluorescence level was still low, when comparing to Tau_{D421} construct, which had the same configuration but a total size of 12.8Kb.

One other major flaw was that cell viability test was done on undifferentiated ReNcells rather than differentiating ReNcells. Cells in the neural progenitor cell state may respond to the same stress vastly different from those in neuronal state would. The reason that it was done in undifferentiated ReNcells was that the test requires standardization of cell count. As differentiation will result in cell death and uneven cell growth in different conditions, cell count standardization would be extremely difficult, if possible. An alternative would be using other neuron-like cells without differentiation, SH-SY5Y cell for example, to perform cell viability test.

2.3 Repeating experiments in HEK cells – Third design iteration

As all experiments in ReNcells were ended prematurely and lack repetition, they were done in HEK cells to back up the observations seen in ReNcells.

There are obviously disadvantages for using HEK cells. Firstly, HEK cells are cancer cells and have a complex karyotype. Second, HEK cells are of kidney origin, though evidences have indicated that HEK cells are more of adrenal neuron origin than typical kidney origin (67,68).

Nevertheless, the reasons for using HEK cells as a substitute are: 1) HEK cells do express neuronal markers, which grant HEK cells some neuronal properties (67,68). 2) HEK cells are not prone to differentiation and can be propagated stably in culture 3) HEK cells do not require differentiation, which shortens the experiment period significantly. 4) HEK cells express genes more robustly, and that will facilitate western blot analysis as well as cell viability test.

2.3.1 Results from the third design iteration

A more comprehensive cell viability test was done, adding sulforaphane as an additional variable (Figure 4). Contrary to that of ReNcell, HEK cell viability was not impacted by pathogenic transgenes. Overexpression or full activation of NRF2 pathway by sulforaphane also did not cause any significant change. These data indicated that HEK cells may not be a good model to test the effectiveness of NRF2 on AD biology.

A test in detecting ROS species was carried out (Figure 5a). This test was done to assess the level of oxidative stress AiP and Tau protein may introduce onto cells. Since sulforaphane is a NRF2 agonist that will fully activate NRF2-related pathway, it was used as a positive control. The result showed that although there was an increase in the amount of ROS species when pathogenic transgenes were incorporated, the induction level was not as high as positive control. Although not as potent as sulforaphane and the differences between

pathogenic transgenes were small, both AiP and Tau were capable of inducing oxidative stress to HEK cells.

Western blots on HEK cell lysates were done with the exact same configuration as ReNcells. The first western blot showed visible bands on all four sulforaphane-stabilized, doxycycline-induced groups (Figure 5b), similar to what was observed in ReNcells. A closer look at all doxycycline-induced samples showed that regardless of the presence of pathogenic genes, all groups had comparable level of NRF2 signals (Figure 5c). This indicated that pathogenic transgenes were not able to activate NRF2 to be noticeable on western blot, even though they were capable of inducing oxidative stress in cells.

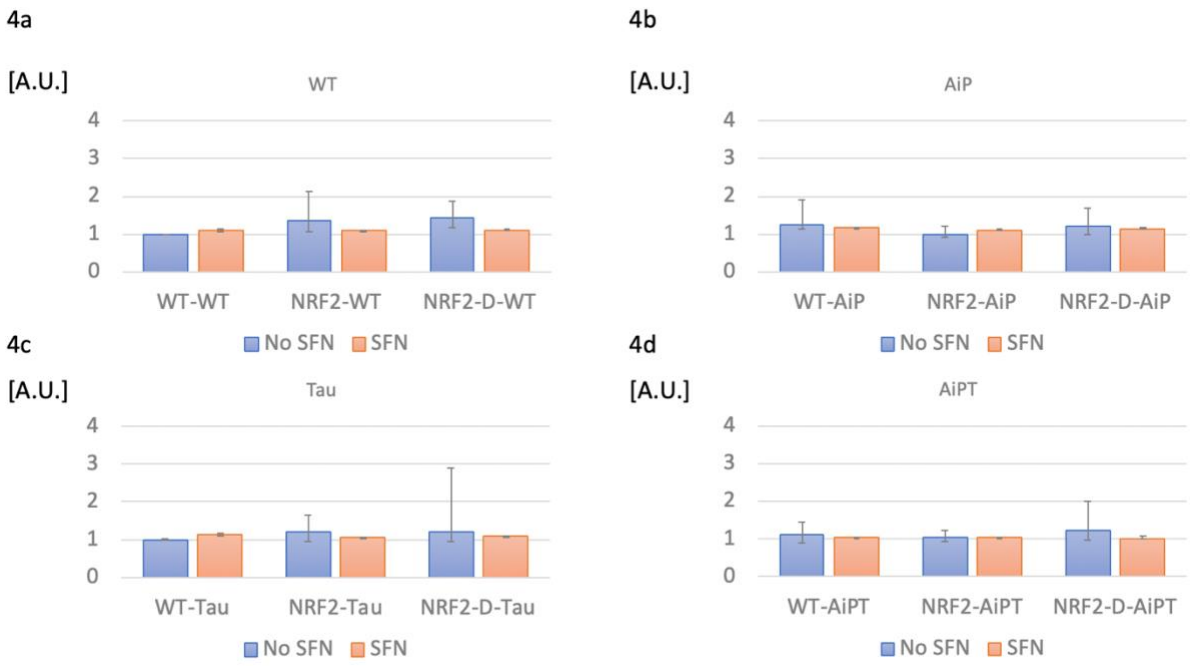

Figure 4. alamarBlue® cell viability test results on HEK cells. Conditions are grouped according to the pathogenic transgene present. Blue bar: groups without SFN. Orange bar: groups with SFN. 4a. no pathogenic transgene. 4b. AiP. 4c. Tau. 4d. AiPT. Arbitrary Units = [A.U.]

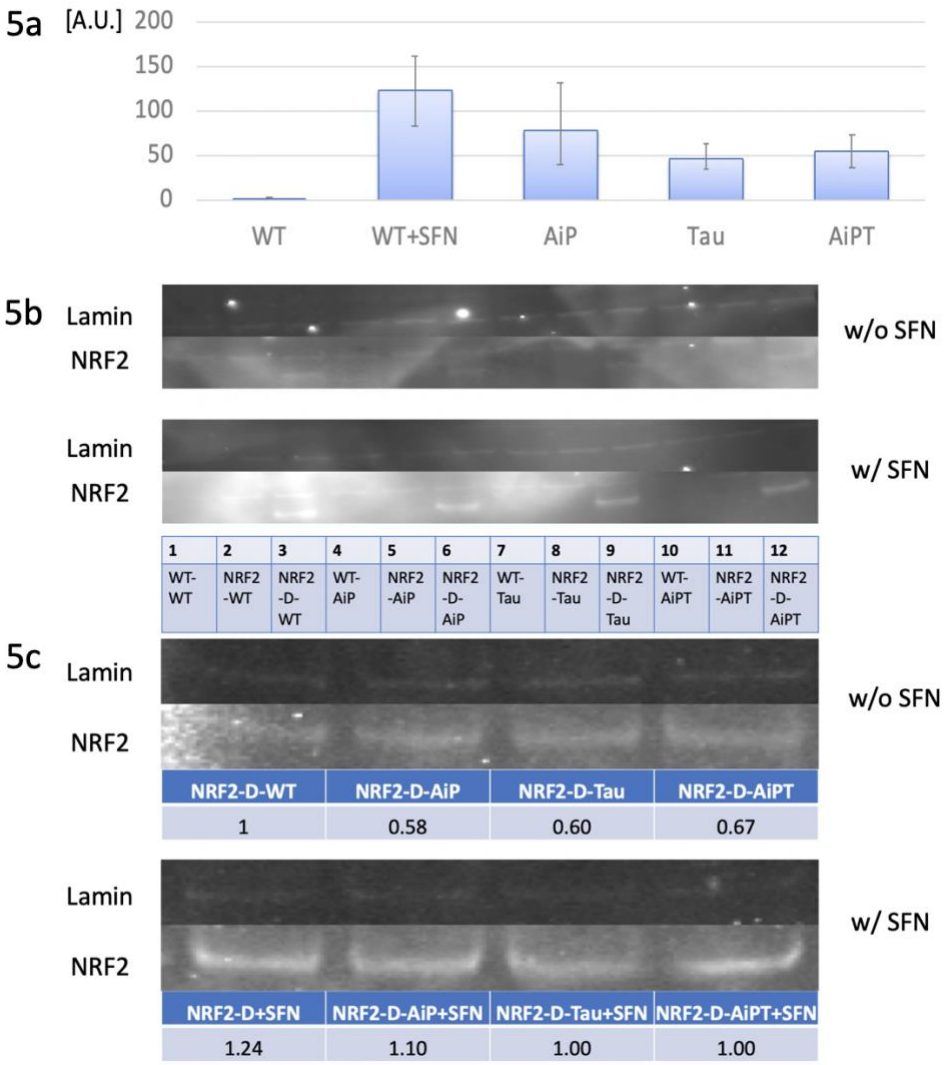

Figure 5. ROS and western blot of HEK cells. 5a: ROS test result. 5b: western blot result of all 12 groups with/without sulforaphane. 5c: western blot result of only doxycycline-induced groups with/without sulforaphane; intensity fold changes are labeled below, normalized to NRF2-D-WT. Arbitrary Units = [A.U.]

Chapter 3 Discussion

In this project, an attempt was made to replicate an *in vitro* AD pathogenic model using human NPC ReNcells and a series of tests were conducted to test the impact of NRF2 on the pathology of the model. Based on all results presented, the conclusions are: 1) Expression of pathological APP and PSEN (AiP) and pathological Tau constructs were able to induce oxidative stress to HEK cells. 2) Although ReNcells saw a trend of enhancing in cell viability with NRF2 overexpression, such observation was not seen in HEK cells. 3) HEK cell viability was not impacted by pathogenic transgenes, and full activation of NRF2 did not have any effect on HEK cell viability.

The initial progression of the project was hindered by author's inexperience. ReNcells handled quite differently from common cell lines like HEK cells or HeLa cells. As author lacked experience working with neuronal cell lines, it costed roughly four months to determine the optimal culture condition to maintain the stemness of ReNcells. Should this process take shorter period, precious time could be saved for further testing and more data could be obtained.

In the future, quite a few can be done to make this project more complete. Firstly, cellular ROS assay should be carried out in SH-SY5Y cells using the configuration described in Table 2. This test will give information on whether pathogenic AiP and/or Tau are capable of inducing oxidative stress in neuronal cells. Subsequently, the impact of pathogenic transgenes on SH-SY5Y cell viability and the effect of NRF2 overexpression in counteracting the impact can be tested in a cell viability test.

All current tests are done in 2-dimensional cultures, of which the biology may be distinctly different from the biology of a 3-dimensional culture. Therefore 3-dimensional ReNcell culture will be created and undergo differentiation for 6 to 12 weeks. The configuration will resemble the one described in Table 2. Those cultures, after differentiation,

will be used for western blot. Western blot of $A\beta_{42}$ and Tau will be done; antibodies targeting total Tau and phosphorylated Tau will be used to better understand the composition of Tau population. Since $A\beta_{42}$ is secreted into the media, an ELISA for $A\beta_{42}$ can be conducted in parallel. Differences between NRF2+Dox groups and WT groups will yield a more definitive conclusion on whether upregulation of NRF2 activity can counteract AD pathology.

Chapter 4 Method & Materials

4.1 cell lines, media and culture conditions

ReNcell VM human neural progenitor cells (ReNcell) were purchased from EMD Millipore (Burlington, MA, USA). The cells were plated on 2X BD Matrigel (BD Biosciences, San Diego, CA)-coated tissue-culture treated 100mm culture dish (EMD Millipore, Burlington, MA). The cells are maintained in stem-cell stage using DMEM/F12, GlutaMAX™ supplement (ThermoFisher Scientific, Waltham, MA) with 2 μg/mL Heparin (StemCell Technologies, Vancouver, Canada), 2% (v/v) B27 neuronal supplement (ThermoFisher Scientific, Waltham, MA), 20 μg/mL EGF (ThermoFisher Scientific, Waltham, MA), 20 μg/mL bFGF (ThermoFisher Scientific, Waltham, MA) and 2% (v/v) Normocin (InvivoGen, San Diego, CA) in a CO_2 culture incubator. The medium was changed the next day after passage and then every 2 days until the cells reached confluency.

For passage, medium was replaced with Accutase (StemCell Technologies, Vancouver, Canada) and incubated for 5 minutes. Detached cell mixture was collected and cell count was measured using a TC10 automated cell counter (Bio-Rad Laboratories, Hercules, CA) and then centrifuged at 200g for 4 minutes to remove supernatant. ~1M cells were plated for continuation.

For differentiation, ReNcells were plated onto BD-Matrigel coated 12-well plates with DMEM/F12, GlutaMAX™ supplement with 2 μg/mL Heparin, 2% (v/v) B27 neuronal supplement and 1% (v/v) penicillin-streptomycin (ThermoFisher Scientific, Waltham, MA) without growth factors. Half of the medium was changed every 3 days for 3 to 4 weeks.

Human embryonic kidney 293T cells (293T cells) were purchased from ATCC (Manassas, VA, USA). The cells were plated directly onto tissue-treated petri dish at about 1M/plate density. Cells are passaged every 4 days using trypsin (ThermoFisher, Waltham, MA).

4.2 DNA constructs

All Tet-inducible constructs were made by replacing the transgenes using Gibson Assembly (New England Biolabs, Ipswich, MA) in a general Lentiviral construct available in the lab. A minimal CMV promoter was followed by a 7-repeat Tet sequence to achieve Tet-inducible feature. Fluorescent proteins (mCherry or Citrine) was placed after an EF1α promoter downstream of the transgenes.

For constitutive constructs, the minimal CMV promoter and Tet repeats were replaced by a PGK promoter by Gibson Assembly (New England Biolabs, Ipswich, MA). EF1α promoter was removed and substituted with a IRES sequence to make the fluorescent protein mCherry under the PGK promoter.

4.3 Viral packaging and viral infection

Lenti-viral constructs were transduced into 293T cells with psPAX2 construct and pCI-VSVG construct from Addgene (Watertown, MA, USA) using FuGene HD Transfection Reagent (Promega, Madison, WI). Medium of the transfected culture was harvested on the third day and fourth day and condensed using Lenti-X concentrator (Takara Bio INC. Kusatsu, Shiga, Japan). Harvested viral particles were aliquoted and subsequently frozen in -80 fridge.

For infection, 5 μL of the original viral solution was added into every well of a 12-well plates; 0.5 μL of the original viral solution was added into every well of a 96-well plates. The plates were incubated for 24 hours and medium was changed. Confirmation of infection was through fluorescent microscopy of mCherry and Citrine.

4.4 qPCR analysis for plasmid gene expression confirmation

Cultures in 6-well plates were lysed with 250 μL TRIzol™ reagent (ThermoFisher Scientific, Waltham, MA) and RNA was extracted using Direct-zol RNA Miniprep kit (Zymo Research, Irvine, CA). cDNA was converted from RNA using a High-Capacity cDNA

Reverse Transcription Kit (ThermoFisher Scientific, Waltham, MA). 0.5 μL of reverse transcription product was used for qPCR using a SYBR™ Green PCR Master Mix (ThermoFisher Scientific, Waltham, MA).

4.5 Flowcytometry analysis

AiP-integrated, mC-integrated and wildtype ReNcells were detached using Accutase (StemCell Technologies, Vancouver, Canada), centrifuged at 200G for 5 minutes, and resuspended with PBS. Cells were briefly stained with Alexa-488-conjugated Sox2 antibody (ThermoFisher Scientific, Waltham, MA) for 15 minutes in PBS and sorted by a FACSAria machine (Sanford Human Stem Cell Core, San Diego, CA). GFP and mCherry chennels were used to detect expression of Sox2 and AiP. 5 million cells were sorted for each genotype.

4.6 Western blot sample preparation & analysis

Cells cultured in 12-well plates were lysed with 150 μL RIPA buffer with DTT (1:1000) and protease inhibitor III (1:200). Lysates were sonicated using sonicater at 20% output for 15 seconds. Protein quantity was standardized using Pierce® BCA Protein Assay Kit – Reducing Agent Compatible (ThermoFisher Scientific, Waltham, MA).

Samples were loaded onto NuPAGE 4%--12% Bis-Tris gels (ThermoFisher Scientific, Waltham, MA) and subsequently transferred to a piece of nitrocellulose membrane (ThermoFisher Scientific, Waltham, MA). Image was captured using Odyssey® CLx imaging system (LI-COR Biosciences, Lincoln, NE). Primary antibodies were used at the following dilution ratio: Lamin A/C antibody (1:1000) (Cell Signaling Technologies, Danvers, MA), NRF2 antibody (1:200) (Santa Cruz Technology, Dallas, TX).

4.7 Cell Viability test

About 10,000 cells were plated into wells of a 96-well plate and incubated at 37 degrees overnight. On the next day, medium was removed and fresh medium containing 10%

alamarBlue® reagent (ThermoFisher Scientific, Waltham, MA) was added. The plate was incubated for 2 hours before analyzing using a microplate reader.

4.8 Cellular ROS assay

About 10,000 cells were plated into wells of a 96-well plate and incubated at 37 degrees overnight. On the next day, cellular ROS level was measured using a Cellular ROS Assay Kit (Abcam, Cambridge, United Kingdom) and a microplate reader.

Bibliography

1. Lane CA, Hardy J, Schott JM. Alzheimer's disease. Eur J Neurol. 2018 Jan;25(1):59–70.

2. Alzheimer's Association. 2016 Alzheimer's disease facts and figures. Alzheimers Dement. 2016 Apr;12(4):459–509.

3. Bahn G, Jo D-G. Therapeutic Approaches to Alzheimer's Disease Through Modulation of NRF2. Neuromolecular Med. 2019 Mar;21(1):1–11.

4. Yatin SM, Varadarajan S, Link CD, Butterfield DA. In vitro and in vivo oxidative stress associated with Alzheimer's amyloid beta-peptide (1-42). Neurobiol Aging. 1999 Jun;20(3):325–30; discussion 339-342.

5. Silva-Palacios A, Ostolga-Chavarría M, Zazueta C, Königsberg M. Nrf2: Molecular and epigenetic regulation during aging. Ageing Res Rev. 2018 Nov;47:31–40.

6. Ma Q. Role of nrf2 in oxidative stress and toxicity. Annu Rev Pharmacol Toxicol. 2013;53:401–26.

7. Ma Q, He X. Molecular basis of electrophilic and oxidative defense: promises and perils of Nrf2. Pharmacol Rev. 2012 Oct;64(4):1055–81.

8. Chan K, Han XD, Kan YW. An important function of Nrf2 in combating oxidative stress: detoxification of acetaminophen. Proc Natl Acad Sci USA. 2001 Apr 10;98(8):4611–6.

9. Kuperstein I, Broersen K, Benilova I, Rozenski J, Jonckheere W, Debulpaep M, Vandersteen A, Segers-Nolten I, Van Der Werf K, Subramaniam V, Braeken D, Callewaert G, Bartic C, D'Hooge R, Martins IC, Rousseau F, Schymkowitz J, De Strooper B. Neurotoxicity of Alzheimer's disease Aβ peptides is induced by small changes in the Aβ42 to Aβ40 ratio. EMBO J. 2010 Oct 6;29(19):3408–20.

10. Binder LI, Frankfurter A, Rebhun LI. The distribution of tau in the mammalian central nervous system. J Cell Biol. 1985 Oct;101(4):1371–8.

11. Johnson GVW, Stoothoff WH. Tau phosphorylation in neuronal cell function and dysfunction. J Cell Sci. 2004 Nov 15;117(Pt 24):5721–9.

12. Caceres A, Kosik KS. Inhibition of neurite polarity by tau antisense oligonucleotides in primary cerebellar neurons. Nature. 1990 Feb 1;343(6257):461–3.

13. Ishihara T, Hong M, Zhang B, Nakagawa Y, Lee MK, Trojanowski JQ, Lee VM. Age-dependent emergence and progression of a tauopathy in transgenic mice overexpressing the shortest human tau isoform. Neuron. 1999 Nov;24(3):751–62.

14. Haase C, Stieler JT, Arendt T, Holzer M. Pseudophosphorylation of tau protein alters its ability for self-aggregation. J Neurochem. 2004 Mar;88(6):1509–20.

15. Abraha A, Ghoshal N, Gamblin TC, Cryns V, Berry RW, Kuret J, Binder LI. C-terminal inhibition of tau assembly in vitro and in Alzheimer's disease. J Cell Sci. 2000 Nov;113 Pt 21:3737–45.

16. Gamblin TC, Chen F, Zambrano A, Abraha A, Lagalwar S, Guillozet AL, Lu M, Fu Y, Garcia-Sierra F, LaPointe N, Miller R, Berry RW, Binder LI, Cryns VL. Caspase cleavage of tau: linking amyloid and neurofibrillary tangles in Alzheimer's disease. Proc Natl Acad Sci USA. 2003 Aug 19;100(17):10032–7.

17. Brothers HM, Gosztyla ML, Robinson SR. The Physiological Roles of Amyloid-β Peptide Hint at New Ways to Treat Alzheimer's Disease. Front Aging Neurosci. 2018;10:118.

18. Hardy JA, Higgins GA. Alzheimer's disease: the amyloid cascade hypothesis. Science. 1992 Apr 10;256(5054):184–5.

19. Hardy J, Selkoe DJ. The amyloid hypothesis of Alzheimer's disease: progress and problems on the road to therapeutics. Science. 2002 Jul 19;297(5580):353–6.

20. Bryan KJ, Lee H, Perry G, Smith MA, Casadesus G. Transgenic Mouse Models of Alzheimer's Disease: Behavioral Testing and Considerations. In: Buccafusco JJ, editor. Methods of Behavior Analysis in Neuroscience [Internet]. 2nd ed. Boca Raton (FL): CRC Press/Taylor & Francis; 2009 [cited 2020 Apr 12]. (Frontiers in Neuroscience). Available from: http://www.ncbi.nlm.nih.gov/books/NBK5231/

21. Okamura N, Yanai K. Brain imaging: Applications of tau PET imaging. Nat Rev Neurol. 2017 Apr;13(4):197–8.

22. Bejanin A, Schonhaut DR, La Joie R, Kramer JH, Baker SL, Sosa N, Ayakta N, Cantwell A, Janabi M, Lauriola M, O'Neil JP, Gorno-Tempini ML, Miller ZA, Rosen HJ, Miller BL, Jagust WJ, Rabinovici GD. Tau pathology and neurodegeneration contribute to cognitive impairment in Alzheimer's disease. Brain. 2017 Dec 1;140(12):3286–300.

23. Braak H, Del Tredici K. Are cases with tau pathology occurring in the absence of Aβ deposits part of the AD-related pathological process? Acta Neuropathol. 2014 Dec;128(6):767–72.

24. Johnson KA, Schultz A, Betensky RA, Becker JA, Sepulcre J, Rentz D, Mormino E, Chhatwal J, Amariglio R, Papp K, Marshall G, Albers M, Mauro S, Pepin L, Alverio J, Judge K, Philiossaint M, Shoup T, Yokell D, Dickerson B, Gomez-Isla T, Hyman B, Vasdev N, Sperling R. Tau positron emission tomographic imaging in aging and early Alzheimer disease. Ann Neurol. 2016 Jan;79(1):110–9.

25. Tönnies E, Trushina E. Oxidative Stress, Synaptic Dysfunction, and Alzheimer's Disease. J Alzheimers Dis. 2017;57(4):1105–21.

26. Beal MF. Mitochondrial dysfunction in neurodegenerative diseases. Biochim Biophys Acta. 1998 Aug 10;1366(1–2):211–23.

27. Swerdlow RH, Burns JM, Khan SM. The Alzheimer's disease mitochondrial cascade hypothesis: progress and perspectives. Biochim Biophys Acta. 2014 Aug;1842(8):1219–31.

28. Webster MT, Pearce BR, Bowen DM, Francis PT. The effects of perturbed energy metabolism on the processing of amyloid precursor protein in PC12 cells. J Neural Transm (Vienna). 1998;105(8–9):839–53.

29. Gasparini L, Racchi M, Benussi L, Curti D, Binetti G, Bianchetti A, Trabucchi M, Govoni S. Effect of energy shortage and oxidative stress on amyloid precursor protein metabolism in COS cells. Neurosci Lett. 1997 Aug 8;231(2):113–7.

30. Gabuzda D, Busciglio J, Chen LB, Matsudaira P, Yankner BA. Inhibition of energy metabolism alters the processing of amyloid precursor protein and induces a potentially amyloidogenic derivative. J Biol Chem. 1994 May 6;269(18):13623–8.

31. Anand P, Singh B. A review on cholinesterase inhibitors for Alzheimer's disease. Arch Pharm Res. 2013 Apr;36(4):375–99.

32. Castro A, Martinez A. Peripheral and dual binding site acetylcholinesterase inhibitors: implications in treatment of Alzheimer's disease. Mini Rev Med Chem. 2001 Sep;1(3):267–72.

33. Olivares D, Deshpande VK, Shi Y, Lahiri DK, Greig NH, Rogers JT, Huang X. N-methyl D-aspartate (NMDA) receptor antagonists and memantine treatment for Alzheimer's disease, vascular dementia and Parkinson's disease. Curr Alzheimer Res. 2012 Jul;9(6):746–58.

34. Greene JG, Greenamyre JT. Bioenergetics and glutamate excitotoxicity. Prog Neurobiol. 1996 Apr;48(6):613–34.

35. Chen H-SV, Lipton SA. The chemical biology of clinically tolerated NMDA receptor antagonists. J Neurochem. 2006 Jun;97(6):1611–26.

36. Wenk GL, Danysz W, Mobley SL. MK-801, memantine and amantadine show neuroprotective activity in the nucleus basalis magnocellularis. Eur J Pharmacol. 1995 Oct 6;293(3):267–70.

37. Miguel-Hidalgo JJ, Alvarez XA, Cacabelos R, Quack G. Neuroprotection by memantine against neurodegeneration induced by beta-amyloid(1-40). Brain Res. 2002 Dec 20;958(1):210–21.

38. Nyakas C, Granic I, Halmy LG, Banerjee P, Luiten PGM. The basal forebrain cholinergic system in aging and dementia. Rescuing cholinergic neurons from neurotoxic amyloid-β42 with memantine. Behav Brain Res. 2011 Aug 10;221(2):594–603.

39. Grossberg GT, Pejović V, Miller ML, Graham SM. Memantine therapy of behavioral symptoms in community-dwelling patients with moderate to severe Alzheimer's disease. Dement Geriatr Cogn Disord. 2009;27(2):164–72.

40. Peskind ER, Potkin SG, Pomara N, Ott BR, Graham SM, Olin JT, McDonald S. Memantine treatment in mild to moderate Alzheimer disease: a 24-week randomized, controlled trial. Am J Geriatr Psychiatry. 2006 Aug;14(8):704–15.

41. Cullinan SB, Gordan JD, Jin J, Harper JW, Diehl JA. The Keap1-BTB protein is an adaptor that bridges Nrf2 to a Cul3-based E3 ligase: oxidative stress sensing by a Cul3-Keap1 ligase. Mol Cell Biol. 2004 Oct;24(19):8477–86.

42. Furukawa M, Xiong Y. BTB protein Keap1 targets antioxidant transcription factor Nrf2 for ubiquitination by the Cullin 3-Roc1 ligase. Mol Cell Biol. 2005 Jan;25(1):162–71.

43. Kobayashi A, Kang M-I, Okawa H, Ohtsuji M, Zenke Y, Chiba T, Igarashi K, Yamamoto M. Oxidative stress sensor Keap1 functions as an adaptor for Cul3-based E3 ligase to regulate proteasomal degradation of Nrf2. Mol Cell Biol. 2004 Aug;24(16):7130–9.

44. Tonelli C, Chio IIC, Tuveson DA. Transcriptional Regulation by Nrf2. Antioxid Redox Signal. 2018 10;29(17):1727–45.

45. Itoh K, Wakabayashi N, Katoh Y, Ishii T, Igarashi K, Engel JD, Yamamoto M. Keap1 represses nuclear activation of antioxidant responsive elements by Nrf2 through binding to the amino-terminal Neh2 domain. Genes Dev. 1999 Jan 1;13(1):76–86.

46. Thimmulappa RK, Mai KH, Srisuma S, Kensler TW, Yamamoto M, Biswal S. Identification of Nrf2-regulated genes induced by the chemopreventive agent sulforaphane by oligonucleotide microarray. Cancer Res. 2002 Sep 15;62(18):5196–203.

47. Wild AC, Moinova HR, Mulcahy RT. Regulation of gamma-glutamylcysteine synthetase subunit gene expression by the transcription factor Nrf2. J Biol Chem. 1999 Nov 19;274(47):33627–36.

48. Vanduchova A, Anzenbacher P, Anzenbacherova E. Isothiocyanate from Broccoli, Sulforaphane, and Its Properties. J Med Food. 2019 Feb;22(2):121–6.

49. Fimognari C, Hrelia P. Sulforaphane as a promising molecule for fighting cancer. Mutat Res. 2007 Jun;635(2–3):90–104.

50. McMahon M, Itoh K, Yamamoto M, Hayes JD. Keap1-dependent proteasomal degradation of transcription factor Nrf2 contributes to the negative regulation of antioxidant response element-driven gene expression. J Biol Chem. 2003 Jun 13;278(24):21592–600.

51. Butterfield DA, Boyd-Kimball D. Oxidative Stress, Amyloid-β Peptide, and Altered Key Molecular Pathways in the Pathogenesis and Progression of Alzheimer's Disease. J Alzheimers Dis. 2018;62(3):1345–67.

52. Fragoulis A, Siegl S, Fendt M, Jansen S, Soppa U, Brandenburg L-O, Pufe T, Weis J, Wruck CJ. Oral administration of methysticin improves cognitive deficits in a mouse model of Alzheimer's disease. Redox Biol. 2017;12:843–53.

53. Dumont M, Wille E, Calingasan NY, Tampellini D, Williams C, Gouras GK, Liby K, Sporn M, Nathan C, Flint Beal M, Lin MT. Triterpenoid CDDO-methylamide improves memory and decreases amyloid plaques in a transgenic mouse model of Alzheimer's disease. J Neurochem. 2009 Apr;109(2):502–12.

54. Wruck CJ, Götz ME, Herdegen T, Varoga D, Brandenburg L-O, Pufe T. Kavalactones protect neural cells against amyloid beta peptide-induced neurotoxicity via extracellular signal-regulated kinase 1/2-dependent nuclear factor erythroid 2-related factor 2 activation. Mol Pharmacol. 2008 Jun;73(6):1785–95.

55. Kanninen K, Malm TM, Jyrkkänen H-K, Goldsteins G, Keksa-Goldsteine V, Tanila H, Yamamoto M, Ylä-Herttuala S, Levonen A-L, Koistinaho J. Nuclear factor erythroid 2-related factor 2 protects against beta amyloid. Mol Cell Neurosci. 2008 Nov;39(3):302–13.

56. Kanninen K, Heikkinen R, Malm T, Rolova T, Kuhmonen S, Leinonen H, Ylä-Herttuala S, Tanila H, Levonen A-L, Koistinaho M, Koistinaho J. Intrahippocampal injection of a lentiviral vector expressing Nrf2 improves spatial learning in a mouse model of Alzheimer's disease. Proc Natl Acad Sci USA. 2009 Sep 22;106(38):16505–10.

57. Zhang J, Zhang R, Zhan Z, Li X, Zhou F, Xing A, Jiang C, Chen Y, An L. Beneficial Effects of Sulforaphane Treatment in Alzheimer's Disease May Be Mediated through Reduced HDAC1/3 and Increased P75NTR Expression. Front Aging Neurosci. 2017;9:121.

58. Hou T-T, Yang H-Y, Wang W, Wu Q-Q, Tian Y-R, Jia J-P. Sulforaphane Inhibits the Generation of Amyloid-β Oligomer and Promotes Spatial Learning and Memory in Alzheimer's Disease (PS1V97L) Transgenic Mice. J Alzheimers Dis. 2018;62(4):1803–13.

59. Jhang KA, Park J-S, Kim H-S, Chong YH. Sulforaphane rescues amyloid-β peptide-mediated decrease in MerTK expression through its anti-inflammatory effect in human THP-1 macrophages. J Neuroinflammation. 2018 Mar 12;15(1):75.

60. Masci A, Mattioli R, Costantino P, Baima S, Morelli G, Punzi P, Giordano C, Pinto A, Donini LM, d'Erme M, Mosca L. Neuroprotective Effect of Brassica oleracea Sprouts Crude Juice in a Cellular Model of Alzheimer's Disease. Oxid Med Cell Longev. 2015;2015:781938.

61. Choi SH, Kim YH, Hebisch M, Sliwinski C, Lee S, D'Avanzo C, Chen H, Hooli B, Asselin C, Muffat J, Klee JB, Zhang C, Wainger BJ, Peitz M, Kovacs DM, Woolf CJ, Wagner SL, Tanzi RE, Kim DY. A three-dimensional human neural cell culture model of Alzheimer's disease. Nature. 2014 Nov 13;515(7526):274–8.

62. APP V717I (London) | ALZFORUM [Internet]. [cited 2020 May 17]. Available from: https://www.alzforum.org/mutations/app-v717i-london

63. APP KM670/671NL (Swedish) | ALZFORUM [Internet]. [cited 2020 May 17]. Available from: https://www.alzforum.org/mutations/app-km670671nl-swedish

64. PSEN1 S290C;T291_S319del (ΔE9Finn) | ALZFORUM [Internet]. [cited 2020 May 17]. Available from: https://www.alzforum.org/mutation/psen1-s290ct291s319del-%CE%B4e9finn

65. Fong H, Hohenstein KA, Donovan PJ. Regulation of Self-Renewal and Pluripotency by Sox2 in Human Embryonic Stem Cells. Stem Cells. 2008 Aug;26(8):1931–8.

66. Qin JY, Zhang L, Clift KL, Hulur I, Xiang AP, Ren B-Z, Lahn BT. Systematic comparison of constitutive promoters and the doxycycline-inducible promoter. PLoS ONE. 2010 May 12;5(5):e10611.

67. Lin Y-C, Boone M, Meuris L, Lemmens I, Van Roy N, Soete A, Reumers J, Moisse M, Plaisance S, Drmanac R, Chen J, Speleman F, Lambrechts D, Van de Peer Y, Tavernier J, Callewaert N. Genome dynamics of the human embryonic kidney 293 lineage in response to cell biology manipulations. Nat Commun. 2014 Sep 3;5:4767.

68. Stepanenko AA, Dmitrenko VV. HEK293 in cell biology and cancer research: phenotype, karyotype, tumorigenicity, and stress-induced genome-phenotype evolution. Gene. 2015 Sep 15;569(2):182–90.